 FDMP, vol.4, no.2, pp.125-137, 2008

Two Dimensional Numerical Simulation of Mixed Convection in a Rectangular Open Enclosure

Md. Tofiqul Islam[1], Sumon Saha[2], Md. Arif Hasan Mamun[3] and Mohammad Ali[4]

Abstract: A numerical study has been performed on mixed convection inside an open cavity on the bottom of a channel. One of the three walls of the cavity experiences a uniform heat flux while the other walls and the top of the channel are adiabatic. Three different cases are considered by applying uniform heat flux on (a) the inflow side (assisting forced flow); (b) the outflow side (opposing forced flow); (c) the bottom horizontal surface (transverse flow). The Galerkin weighted residual method of finite element formulation is used to discretize the governing equations. For mixed convection, the influential parameters are the Grashof number (*Gr*), Richardson number (*Ri*) and Reynolds number (*Re*) by which different fluid and heat transfer characteristics inside the cavity are obtained. In the present study, velocity vectors, streamlines, isotherms, non-dimensional vertical velocities, maximum non-dimensional heated wall temperature and average Nusselt number of the heated wall are reported for Ri = 0.1 to 100, Re = 100 and the ratio of channel and cavity heights (H/D) with the range of 0.1 to 1.5. With the increase of Richardson numbers, the convective heat transfer becomes predominant over the conduction heat transfer. From the computation, it is observed that the higher heat transfer occurs for opposing forced flow situation at low Richardson number. For higher Richardson number, a better thermal performance is achieved for the transverse flow case.

[1] Lecturer, Bangladesh University of Engineering & Technology (BUET), Dhaka, Bangladesh
[2] Lecturer, Bangladesh University of Engineering & Technology (BUET), Dhaka, Bangladesh
[3] Assistant Professor, Bangladesh University of Engineering & Technology (BUET), Dhaka, Bangladesh
[4] Professor, Bangladesh University of Engineering & Technology (BUET), Dhaka, Bangladesh

Keyword: Mixed convection, Richardson number, assisting forced flow, opposing forced flow, transverse flow.

Nomenclature

C_p	specific heat of the fluid at constant pressure ($\mathrm{Jkg^{-1}K^{-1}}$)
g	gravitational acceleration ($\mathrm{ms^{-2}}$)
Gr	Grashof number, $g\beta qD^4/k\upsilon^2$
h	convective heat transfer coefficient ($\mathrm{Wm^{-2}K^{-1}}$)
H	height of the channel opening (m)
D	height of the enclosure (m)
k	thermal conductivity ($\mathrm{Wm^{-1}K^{-1}}$)
Nu	Nusselt number, hD/k
p	pressure ($\mathrm{Nm^{-2}}$)
P	nondimensional pressure, $p/\rho u_i^2$
Pr	Prandtl number, υ/α
q	heat flux ($\mathrm{Wm^{-2}}$)
Re	Reynolds number, u_iD/υ
Ri	Richardson number, Gr/Re^2
T	temperature (K)
u, v	velocity components ($\mathrm{ms^{-1}}$)
U, V	nondimensional velocity components, u/u_i, v/u_i
x, y	cartesian coordinates (m)
X, Y	nondimensional cartesian coordinates, x/D, y/D
L	length of the enclosure (m)
L_e	exit length of the channel (m)
L_s	length of the heated wall (m)
S	direction of the heated strip
R^2	maximum correlation coefficient

Greek symbols

α	thermal diffusivity, $k/\rho C_p$ ($\mathrm{m^2s^{-1}}$)
β	thermal expansion coefficient, $-(1/\rho)(\partial\rho/\partial t)_p$ ($\mathrm{K^{-1}}$)

θ nondimensional temperature, $(T-T_i)/(qD/k)$
υ kinematic viscosity of the fluid (m^2s^{-1})
ρ density of the fluid (kgm^{-3})
Φ angle of attack (degree)

Subscripts

i inlet state
max maximum
av average

1 Introduction

A number of practical situations such as nuclear reactors, solar collectors, crystal growth, and cooling of electronic devices, involve convective heat transfer, which is neither forced nor free in nature. This phenomenon arises when a fluid is forced to flow over a heated surface even though at a low velocity. The forced flow velocity is coupled with convective velocity generated by the buoyancy forces resulting from a reduction in fluid density near the heated surface. As a relevant example of this type of flow, the reader may consider the mother board of a computer with many integrated circuits acting as heat sources and generating heat to be removed by both natural convection and induced flow of air. The ratio Gr/Re^2 gives a qualitative indication of the influence of buoyancy on forced convection, and when the Grashof number is of the same order of magnitude or larger than the square of the Re, free convection effects cannot be ignored, compared to forced convection. In the region where both free and forced convection effects are of the same order of magnitude, heat transfer is increased by buoyancy effects acting in the direction of flow and decreased when acting in the opposite direction.

1.1 Literature review

For the case of pure buoyancy convection the reader may consider Lappa (2005), Melnikov and Shevtsova (2005), Punjabi, Muralidhar and Panigrahi (2006), Sohail and Saghir (2006). Oosthuizen and Paul (1985) studied the problem of mixed convection flow in a cavity where one of the side walls was heated uniformly and the horizontal wall was adiabatic, particularly the interaction of forced flow and buoyancy flow. They used a Galerkin finite element method for numerical solution. Vafai and Ettefagh (1990); Vafai, Desai, Iyer and Dyko (1997); and Khanafer and Vafai (2000) investigated the thermal field and flow field inside the cavity and near the surrounding walls with varying aspect ratio for both assisting and opposing forced flow cases. Papanicolaou and Jaluria (1990) studied numerically the mixed convection within a rectangular enclosure with an isolated heat source experiencing a constant heat flux. They found that the Nusselt number increased as Richardson number increased while the Reynolds number remained fixed. Also the Nusselt number increased as the Reynolds number increased at a particular value of Richardson number. Again Papanicolaou and Jaluria (1993) studied numerically the interaction of buoyancy induced flow from an isolated heat source with an externally induced flow stream inside an enclosure. They found that the heat transfer from the source was higher if the conductivity of the solid was higher. The highest average Nusselt number was obtained for the heat source locating bottom. In Hsu and Wang (2000) the heat source was isolated and positioned at the mid of the cavity by a vertical board. They found results in line with those obtained by Papanicolaou and Jaluria (1990). Khanafer, Vafai, Lightstone (2002) numerically studied mixed convection in an open ended enclosure for three different angles of attack of the inlet flow. For $\Phi = 90^o$ the average Nusselt number of the upper horizontal wall was highest and became lowest for $\Phi = 45^o$. Omri, Ben Nasrallah (1999) performed numerical analysis on mixed convection in a cavity where the inlet and outlet channels were fixed diagonally ascending or descending order. Fluid was injected at lower temperature than the initial temperature of the cavity. They noticed that for Ri = 0.1 to 10 and Re = 10 to 100, the average temperature at the exit was higher in the descending mode and air injected from the bottom of the hot wall was more effective for the removal of heat. Hsu, Pao-Tung Hsu, Sey-Ping How (1997) indicated that the average Nusselt number increased

as Reynolds number increased at a fixed Richardson number. A better cooling system was designed by placing the heat source close to cold inlet stream.

2 Physical Model

Fig. 1. shows the three dimensional view of the geometry under consideration: an open cavity interacting with a channel, as shown in Fig. 2. Here one wall of the rectangular cavity is heated by a uniform heat flux and the other walls remain adiabatic. Flow enters through the left opening of the channel at a uniform velocity, u_i. The inlet flow is assumed to have an ambient temperature, T_i (i.e. non-dimensional inlet temperature, $\theta_i = 0$) and a zero diffusion flux is assumed at the channel exit (outflow boundary conditions). Flow in the cavity is assumed to be two dimensional, laminar and incompressible with negligible viscous dissipation and a Boussinesq fluid. Here H/D is ventilation ratio (i.e. the ratio of the height of the inlet flow channel to the height of the rectangular cavity) and L/D is the cavity aspect ratio.

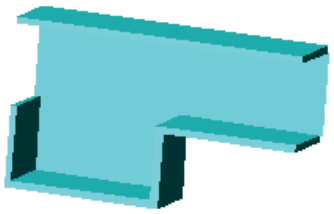

Figure 1: 3D cross-sectional view of an open cavity at the bottom of a rectangular channel

2.1 Mathematical Modeling

Using the Boussinesq approximation and neglecting the viscous dissipation effect and compressibility effect, the governing equations for 2D laminar, incompressible flow are written as follows:

Continuity Equation

$$\frac{\partial u}{\partial x}+\frac{\partial v}{\partial y}=0 \tag{1}$$

x-momentum Equation

$$u\frac{\partial u}{\partial x}+v\frac{\partial u}{\partial y}=-\frac{1}{\rho}\frac{\partial p}{\partial x}+\upsilon\left(\frac{\partial^2 u}{\partial x^2}+\frac{\partial^2 u}{\partial y^2}\right) \tag{2}$$

y-momentum Equation

$$u\frac{\partial v}{\partial x}+v\frac{\partial v}{\partial y}=-\frac{1}{\rho}\frac{\partial p}{\partial y}+\upsilon\left(\frac{\partial^2 v}{\partial x^2}+\frac{\partial^2 v}{\partial y^2}\right)+g\beta\left(T-T_i\right) \tag{3}$$

Energy Equation

$$u\frac{\partial T}{\partial x}+v\frac{\partial T}{\partial y}=\frac{k}{\rho C_p}\left(\frac{\partial^2 T}{\partial x^2}+\frac{\partial^2 T}{\partial y^2}\right) \tag{4}$$

The governing equations in non dimensional form can be written by using the following non dimensional variables and parameters.

$$X=\frac{x}{D} \qquad Y=\frac{y}{D} \qquad \theta=\frac{T-T_i}{\left(\frac{qD}{k}\right)}$$

$$U=\frac{u}{u_i} \qquad V=\frac{v}{u_i} \qquad \mathrm{P}=\frac{p}{\rho u_i^2}$$

$$Re=\frac{u_i D}{\upsilon} \qquad Gr=\frac{\beta g q D^4}{\upsilon^2 k} \qquad Pr=\frac{\upsilon}{\alpha}$$

Non-dimensional Continuity Equation

$$\frac{\partial U}{\partial X}+\frac{\partial V}{\partial Y}=0 \tag{5}$$

Non-dimensional X-momentum Equation

$$U\frac{\partial U}{\partial X}+V\frac{\partial U}{\partial Y}=-\frac{\partial P}{\partial X}+\frac{1}{Re}\left(\frac{\partial^2 U}{\partial X^2}+\frac{\partial^2 U}{\partial Y^2}\right) \tag{6}$$

Non-dimensional Y-momentum Equation

$$U\frac{\partial V}{\partial X}+V\frac{\partial V}{\partial Y}=-\frac{\partial P}{\partial Y}+\frac{1}{Re}\left(\frac{\partial^2 V}{\partial X^2}+\frac{\partial^2 V}{\partial Y^2}\right)+\frac{Gr}{Re^2}\theta \tag{7}$$

Non-dimensional Energy equation

$$U\frac{\partial \theta}{\partial X}+V\frac{\partial \theta}{\partial Y}=\frac{1}{RePr}\left(\frac{\partial^2 \theta}{\partial X^2}+\frac{\partial^2 \theta}{\partial Y^2}\right) \tag{8}$$

The average Nusselt number is calculated as

$$Nu_{av}=\frac{1}{L_s}\int_0^{L_s}\frac{h(s)s}{k}ds \tag{9}$$

where L_s is the length of the heated wall and $h(s)$ is the local convection heat transfer coefficient of the heated wall.

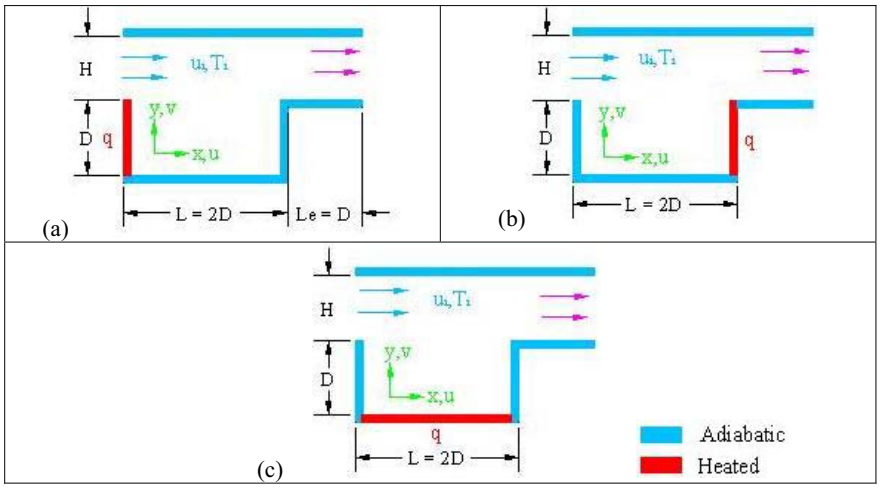

Figure 2: Physical model of three cases of heating: (a) assisting forced flow, (b) opposing forced flow, (c) transverse flow

Non-dimensional average Nusselt Number is

$$Nu_{av} = \frac{1}{L_s/D}\int_0^{L_s/D} \frac{S}{\theta} dS \tag{10}$$

where S is the dimensionless position of heated strip (may either along X direction or Y direction).

2.2 Boundary Conditions

(1) No slip condition at all walls

$$U = 0, \quad V = 0; \quad \begin{cases} Y = 0, & 0 \le X \le 2 \\ X = 0, & 0 \le Y \le 1 \\ X = 2, & 0 \le Y \le 1 \\ Y = 1, & 2 \le X \le 4 \\ Y = 1 + H/D, & 0 \le X \le 4 \end{cases} \tag{11}$$

(2) Uniform heat flux is applied to one of walls of cavity while others remain adiabatic

$$\frac{\partial \theta}{\partial S} = -1 \begin{cases} X = 0, \quad 0 \le Y \le 1 \\ \text{(assisting forced flow)} \\ X = 2, \quad 0 \le Y \le 1 \\ \text{(opposing forced flow)} \\ Y = 0, \quad 0 \le X \le 2 \\ \text{(transverse flow)} \end{cases}$$

$$\frac{\partial \theta}{\partial X} = 0 \quad \text{or}$$

$$\frac{\partial \theta}{\partial Y} = 0 \begin{cases} Y = 0,\ 0 \le X \le 2;\ X = 2,\ 0 \le Y \le 1 \\ \text{(assisting forced flow)} \\ X = 0,\ 0 \le Y \le 1;\ Y = 0,\ 0 \le X \le 2 \\ \text{(opposing forced flow)} \\ X = 2,\ 0 \le Y \le 1;\ X = 0,\ 0 \le Y \le 1 \\ \text{(transverse flow)} \end{cases} \tag{12}$$

(3) Incoming flow has uniform velocity along x coordinate and ambient temperature

$$\theta = 0, \quad U = 1, \quad V = 0; \quad \text{at} \quad X = 0,\ 1 \le Y \le H/D \tag{13}$$

(4) Outflow has zero diffusion flux

$$\partial\theta/\partial X = 0; \quad \text{at} \quad X = 4,\ 1 \le Y \le H/D \tag{14}$$

3 Numerical Procedure

The numerical procedure is based on the Galerkin weighted residual method (finite element formulation). The approximation functions used in

the Galerkin method are of higher order polynomial. The governing equations are linearized and solved by segregated solution method. The conjugate residual scheme is used to solve the symmetric pressure type equation systems, while the conjugate gradient squared is used for the non-symmetric advection diffusion type equations. The matrix factorization technique (LU decomposition) is used with partial pivoting. An interpolation function is used over the generic element and expresses the variation of the field variable inside the element with respect to the global reference axes, which are defined for the entire domain.

3.1 Grid Independency Test

Preliminary results have been are obtained to assess grid independency. Test for grid accuracy has been done for the arrangements of five different non regular grid systems with the following number of nodes in the rectangular cavity: 17846, 29754, 36046, 45819 and 54139.The results are reported on the Tab. 1. It is found that 45819 non regular nodes are sufficient to provide accurate results.

3.2 Code Validation

The computer code has been validated with the results obtained for mixed convection in a channel with an open cavity as obtained by Manca, Nardini, Khanafer and Vafai (2003). The comparison of the results is reported in the Tab. 2. From the comparison it can be seen that the computer code is capable of calculating the flow field in the present configuration.

4 Results and Discussion

Several significant parameters such as Reynolds number, Richardson number and ventilation ratio of the enclosure are investigated here for a rectangular cavity with $L/D = 2$. These ranges are varied as $Re = 100$, $0.1 \leq Ri \leq 100$ and $0.1 \leq H/D \leq 1.5$. Only the figures showing significant changes in thermo-fluid dynamic fields are presented here.

4.1 Flow and Thermal field characteristic

4.1.1 Effect of Richardson number

The effect of Richardson number on the flow and thermal fields within an open cavity of $H/D = 1$ and $Re = 100$ for the assisting forced flow case is presented in Fig. 3. For a relatively small Richardson number ($Ri = 0.1$), a small weak recirculation exists inside the cavity. Buoyancy effect in the cavity is weak and diffusion is the principal mode of heat transfer. The isotherms are clustered near the heated wall, indicating heat transfer via conduction is dominant. As Ri increases, the intensity of the recirculating cell rises up. Thereby natural convective current becomes stronger for $Ri = 100$ a thermal buoyancy layer develops near the heated wall; a horizontal thermal plume is formed near the upper boundary of the cavity. Both these features indicate that heat transfer occurs mostly via convection.

Fig. 4 shows the flow and isothermal patterns for $H/D = 1$ and $Re = 100$ in case of opposing forced flow. At low values of Ri, a single circulating cell is formed. With an increase of Ri, the large circulating cell is squeezed by penetration of the forced flow. As shown in the first frame of Fig. 4, for $Ri = 0.1$ heat transfer is governed by diffusion and by the weak circulating cell induced by the external flow. For $Ri = 100$, a rising strong flow appears near the heated wall. This strong flow is driven by the joint actions of the buoyancy and the forced flow that for such conditions penetrates significantly into the cavity. A thermal boundary layer is clearly visible near the right wall of the cavity and a thermal plume transported by the forced wind is present in the channel. The changes in flow and thermal behaviors within a cavity, subjected to transverse heating, for different Richardson number are shown in Fig. 5. At lower value of Richardson number, the buoyancy effect is overwhelmed by the effect of the induced air flow. A recirculating cell of little strength is formed inside the cavity. The strength of circulating cell becomes higher along with Richardson number and natural convective current is set over the conduction. The isotherms are almost linear indicating that the heat transfer is carried

Table 1: Comparison of the results for various grid dimensions ($Re = 100$, $Ri = 1$, $H/D = 1$)

No. of Nodes	17846	29754	36046	45819	54139
Nu_{av}	1.910	2.015	2.016	2.017	2.017
θ_{max}	0.890	0.860	0.860	0.859	0.859

Table 2: Comparison of the results for validations at $Re = 100$, $H/D = 1$ and $Pr = 0.7$

Heating Mode	Governing parameters	Present work		Work of Manca, Nardini, Khanafer and Vafai (2003)	
		$Ri = 0.1$	$Ri = 100$	$Ri = 0.1$	$Ri = 100$
Assisting forced flow	Nu_{av}	1.686713	3.101788	1.5	-
	θ_{max}	0 .546469	0.210459	0.544	0.209
Opposing forced flow	Nu_{av}	1.765711	4.065624	1.78	-
	θ_{max}	0.626651	0.132072	0.627	0.132
Transverse flow	Nu_{av}	1.633	3.71892	1.65	-
	θ_{max}	1.066	0.440359	1.06	0.437

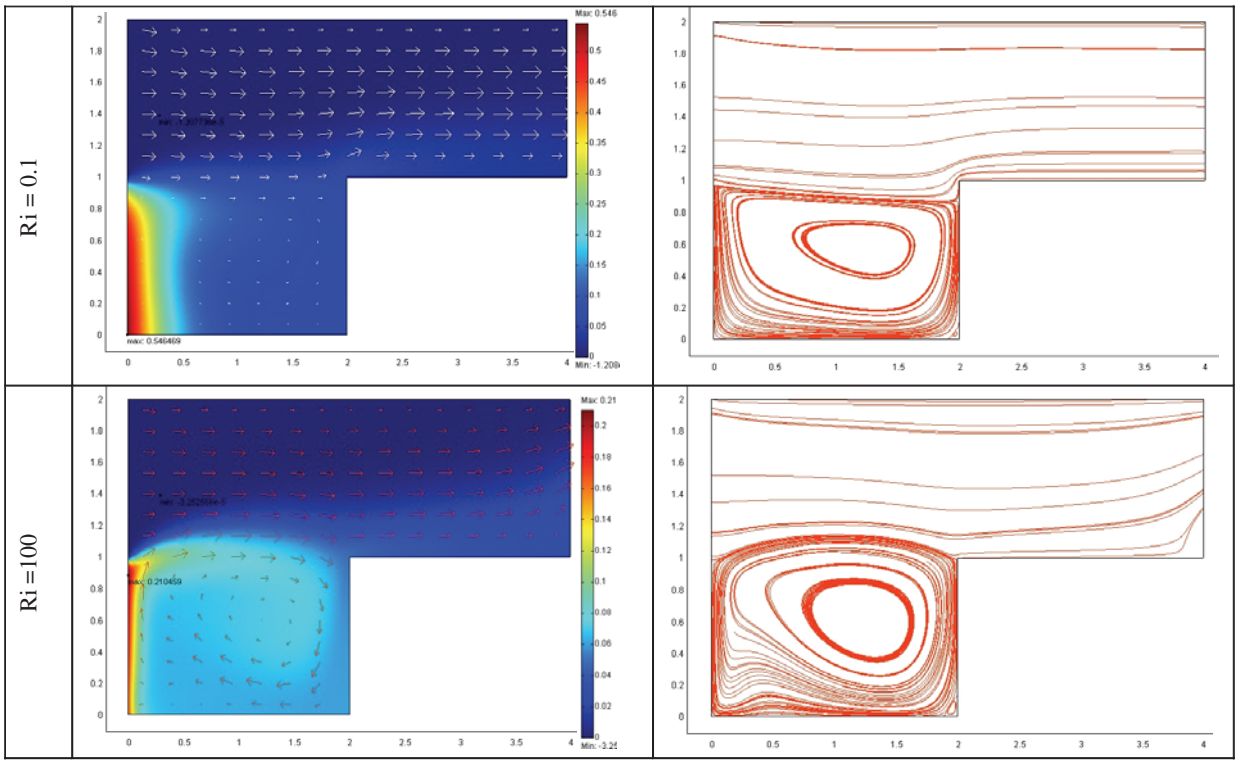

Figure 3: Effect of Richardson number on the velocity vectors, the isotherms and the streamlines for assisting forced flow ($H/D = 1$, $Re = 100$)

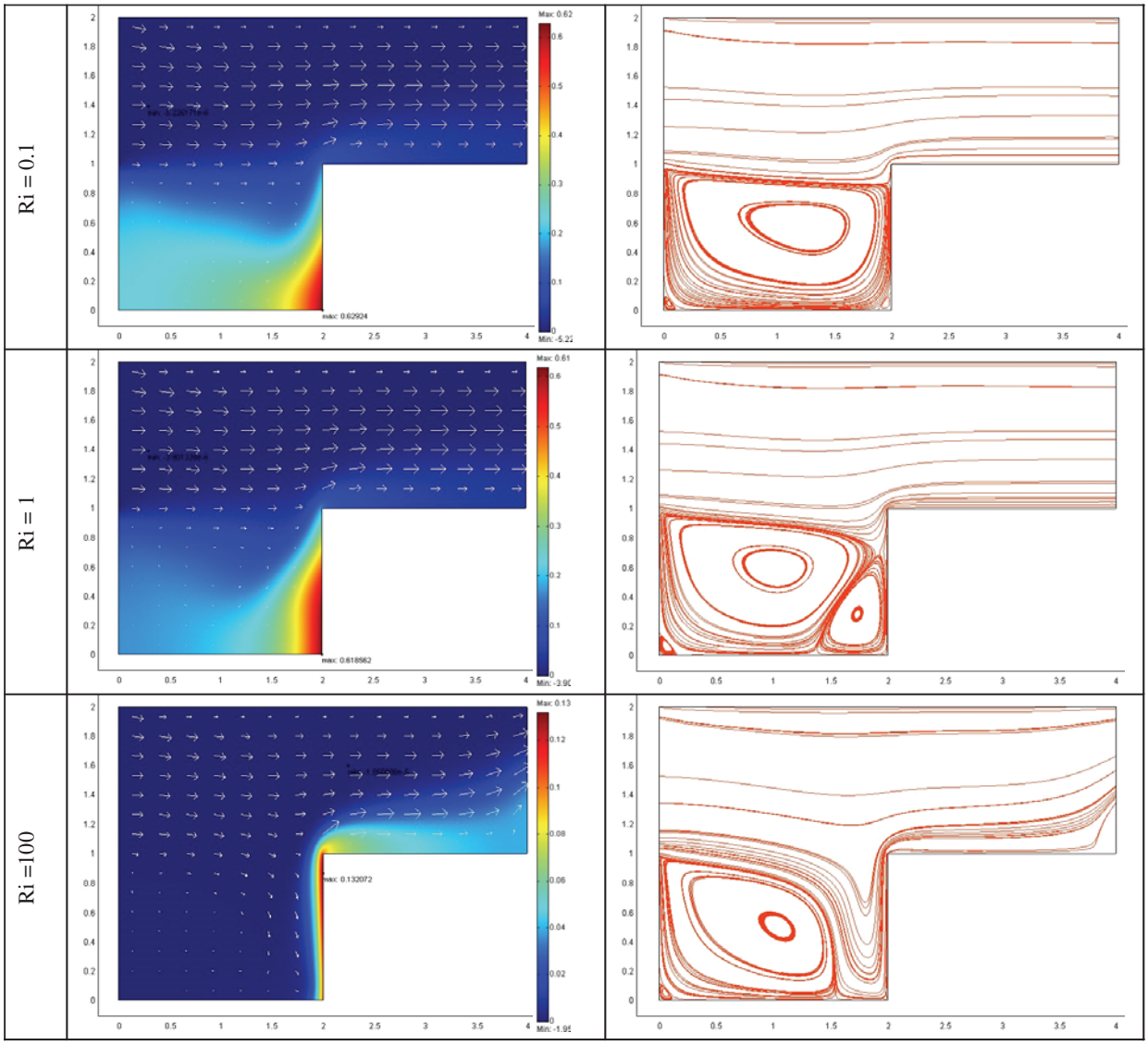

Figure 4: Effect of Richardson number on the velocity vectors, the isotherms and the streamlines for opposing forced ($H/D = 1$, $Re = 100$)

out mainly by conduction for the lower values of Ri. As Richardson number increases, nonlinear isotherms become visible throughout the cavity showing dominance of the buoyancy-driven natural convection.

4.1.2 Effect of ventilation ratio

The effect of different ventilation ratios on the the streamlines and isotherms for assisting and opposing forced flow is shown in Fig. 6 and 7 respectively.

4.2 Velocity and temperature distribution

Fig. 8 shows the non-dimensional vertical velocity profiles for different values of ventilation ratio while considering $Y = 0.5$, $Ri = 1$ and $Re = 100$ for the three heating cases considered in the present work. It is observed that two recirculating cells of opposite rotational directions and different intensity are formed. A vortex grows at the vicinity of the left adiabatic side wall for higher values of H/D both for opposing forced flow and transverse flow cases. But the strength of the circulating cell in the transverse heating configuration is higher

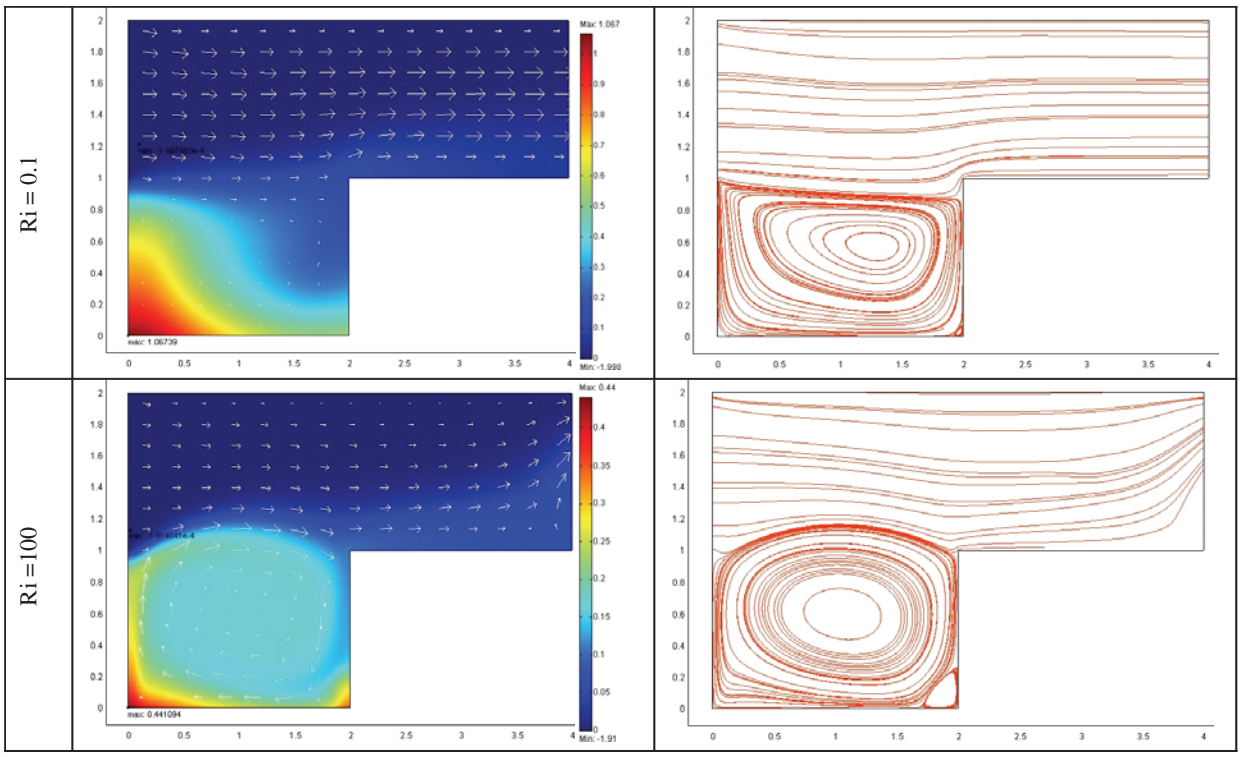

Figure 5: Effect of Richardson number on the velocity vectors, the isotherms and the streamlines for transverse flow (H/D = 1, Re = 100)

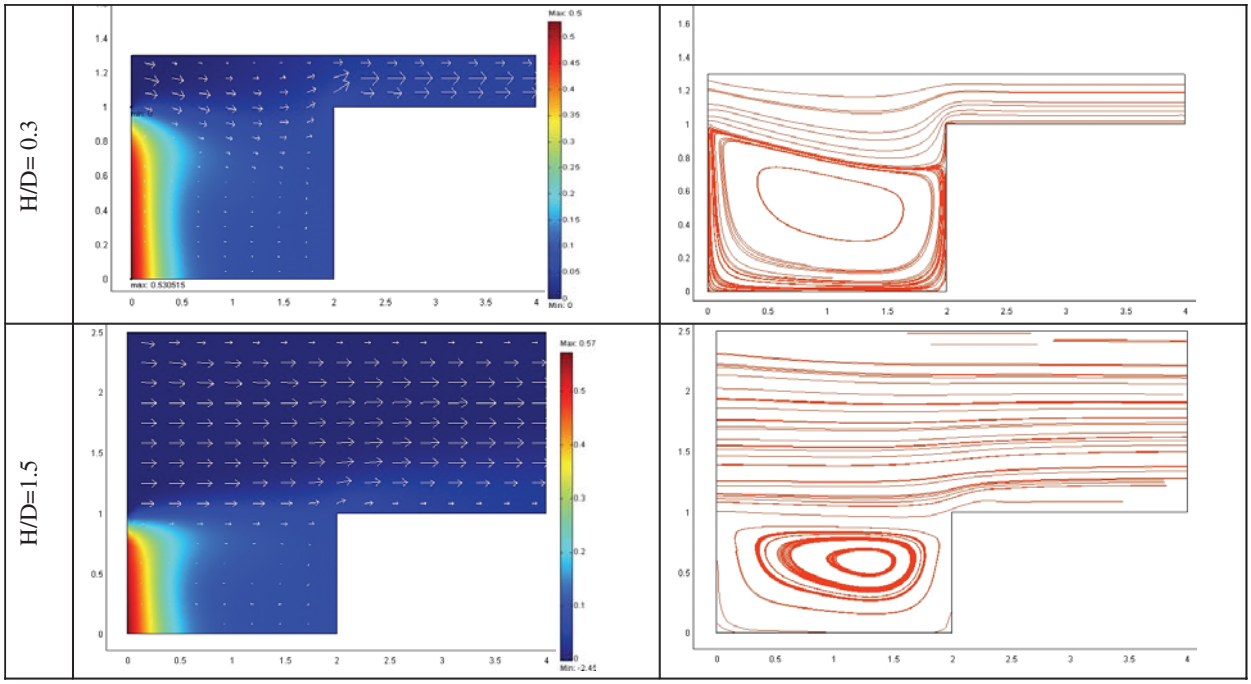

Figure 6: Velocity vectors, isotherms and streamlines for assisting forced flow at various ventilation ratio, H/D (Ri = 0.1, Re = 100)

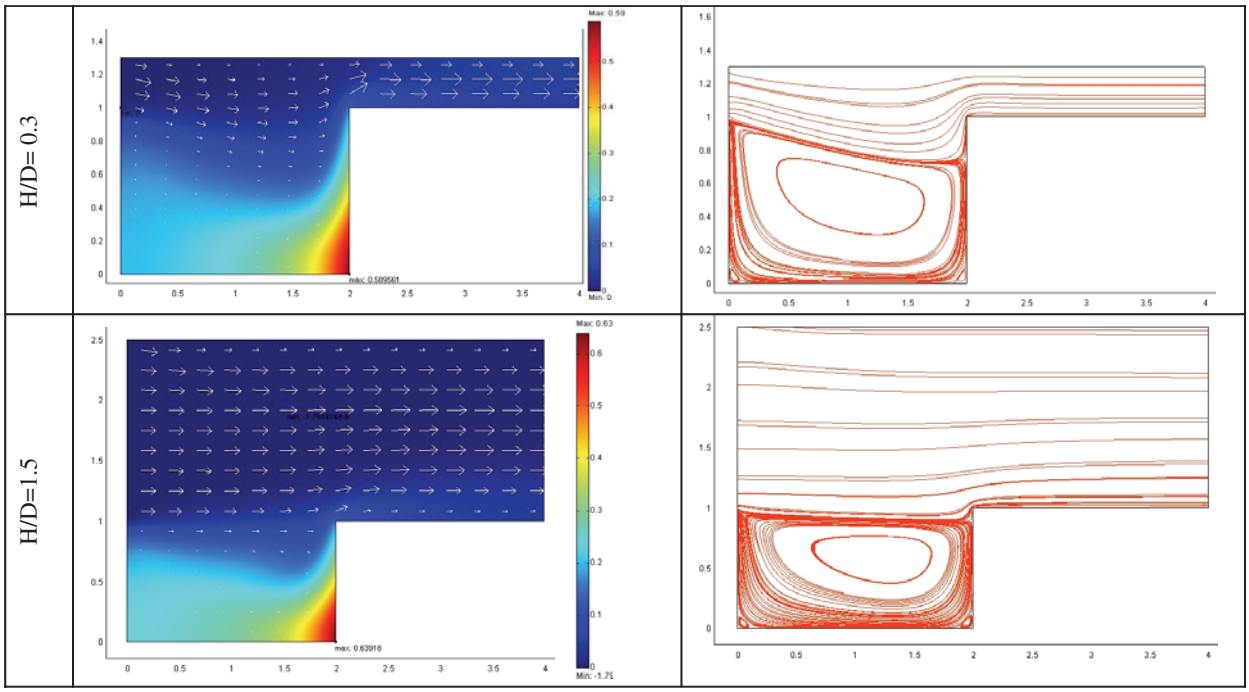

Figure 7: Velocity vectors, isotherms and streamlines for opposing forced flow at various ventilation ratio, H/D (Ri = 0.1, Re = 100)

than that for the opposing forced flow case. Thus the convective heat transport mechanism is dominating for the transverse flow model. The influence of different Richardson numbers on the non-dimensional vertical velocity profiles for H/D = 0.5 is shown in Fig. 9. A low value of Richardson number leads to a similar flow patterns for all the three cases. In case of assisting forced flow, it is noticeable that three sub-vortices are formed at higher Ri resulting in hindrance of heat transfer process. From the investigation on the opposing forced flow case, it is noticed that when the Richardson number increases, the depth of penetration of the induced flow decreases due to the buoyancy force. Thus heat transfer is enhanced. In case of transverse flow, the strength of circulation becomes higher compared to the opposing forced flow case. Thereby optimum thermal performance is obtained while H/D is fixed to 0.5.

4.3 Heat transfer performance

In electronic component cooling applications, the maximum temperature on the surface is a critical issue since it may become detrimental to the circuitry if too high. It is therefore of interest to examine the maximum temperature at the heated wall. The variation of the maximum dimensionless temperature on the heated surface with Richardson number for all the three heating cases considered here is presented in Fig. 10. In general, θ_{max} decreases with increasing Richardson number. This is due to the fact that the local Nusselt number S/θ shown in Eq. 10, is reciprocal of the non-dimensional surface temperature for uniform heat flux condition. The maximum non-dimensional temperature decreases much more rapidly at Richardson number of order 1 or greater for the opposing forced flow and transverse flow cases. The strong buoyancy force is responsible for this type of thermal scenario.

Fig. 11 (a) and (b) shows the effect of different ventilation ratio on the maximum dimensionless temperature and average Nusselt number for the three different thermal models. It also presents the comparison of the results obtained by the present study and the investigation of Manca, Nardini, Khanafer and Vafai (2003). The results of the present investigation has close agreement to that

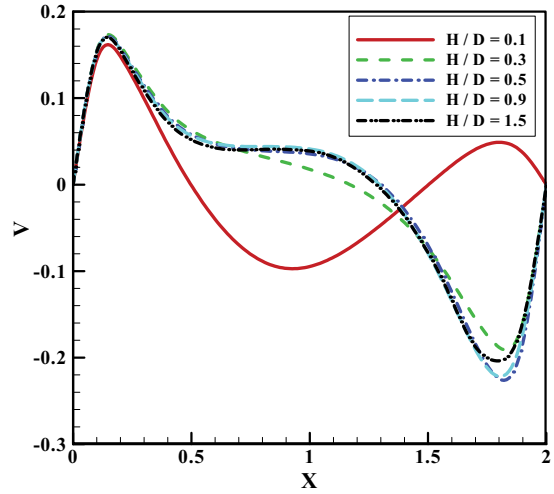

(a)

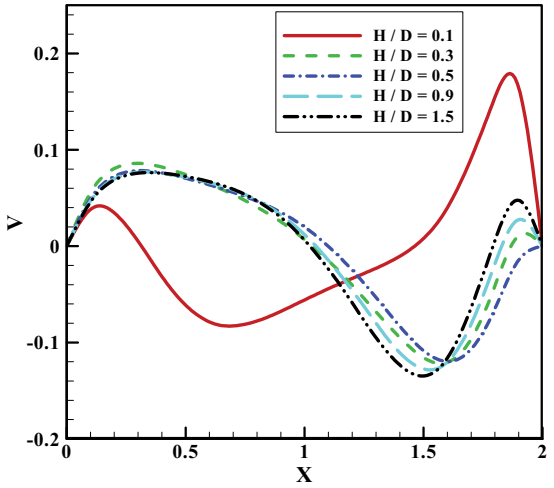

(b)

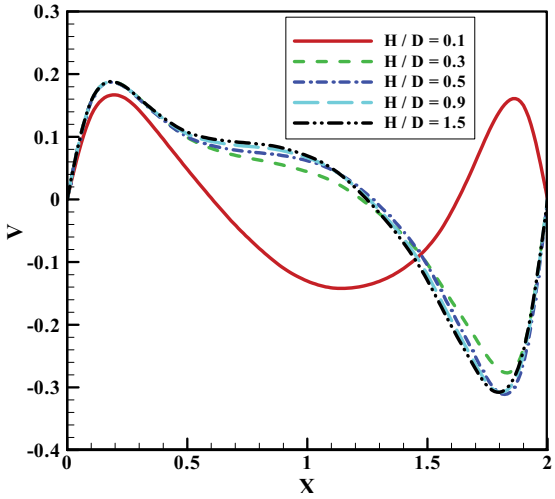

(c)

Figure 8: Non-dimensional vertical velocity for different ratio of H/D at $Y = 0.5$, $Ri = 1$ and $Re = 100$, observed for the cases: (a) Assisting forced flow, (b) Opposing forced flow, (c) Transverse flow

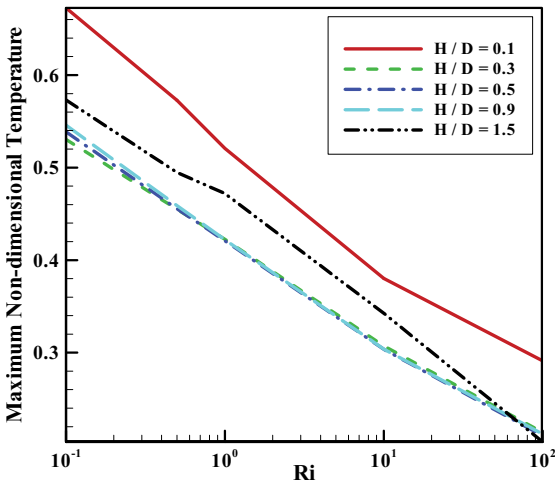

(a)

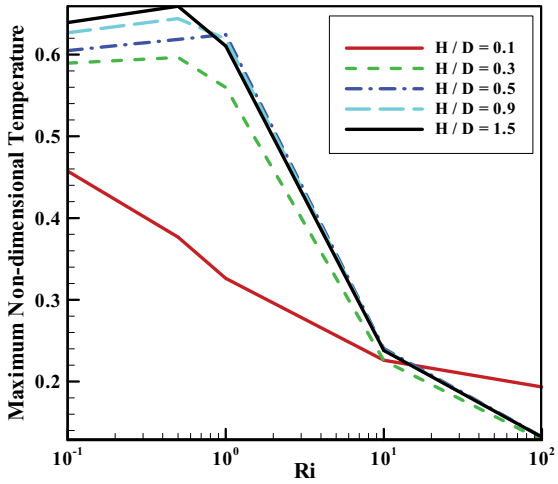

(b)

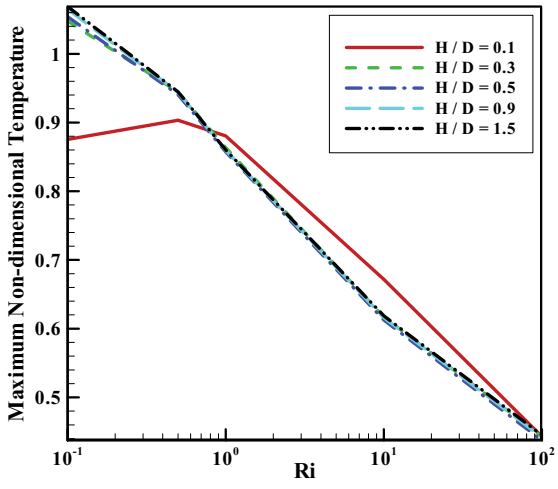

(c)

Figure 10: The effect of maximum non-dimensional temperature for varying Ri for (a) Assisting forced flow, (b) Opposing forced flow, (c) Transverse flow while $Re = 100$

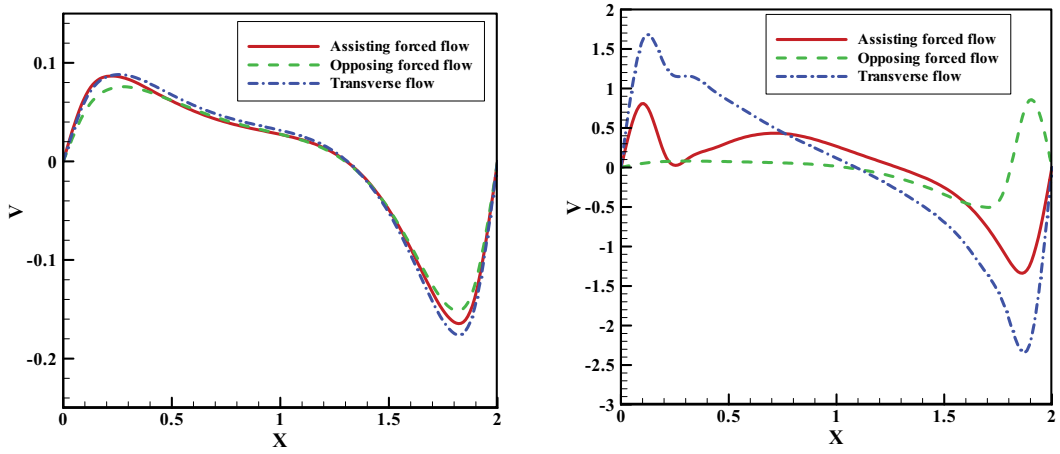

Figure 9: Non-dimensional vertical velocity for three different cases at $H/D = 0.5$, $Y = 0.5$, $Re = 100$ and (a) $Ri = 0.1$, (b) $Ri = 100$

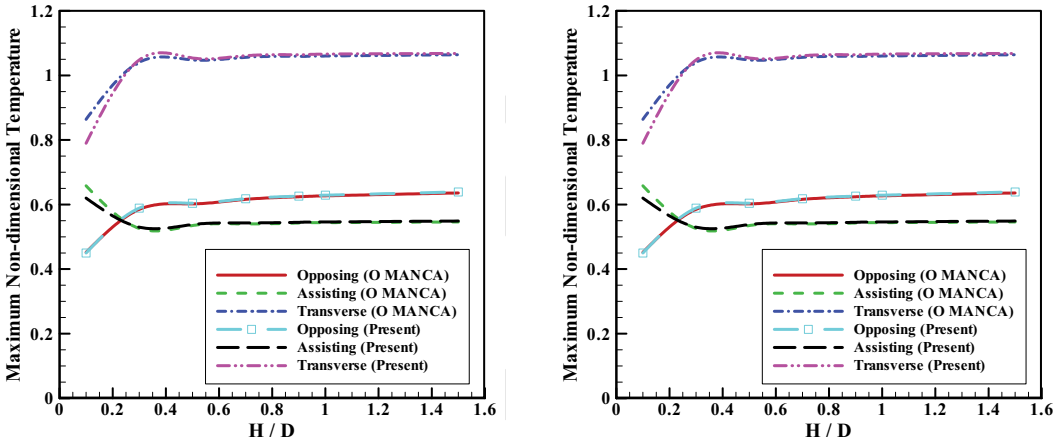

Figure 11: Comparison of the maximum temperature variation between the present work and O'MANCA work for assisting forced flow, opposing forced flow and transverse flow for various H/D ($Ri = 0.1$, $Re = 100$)

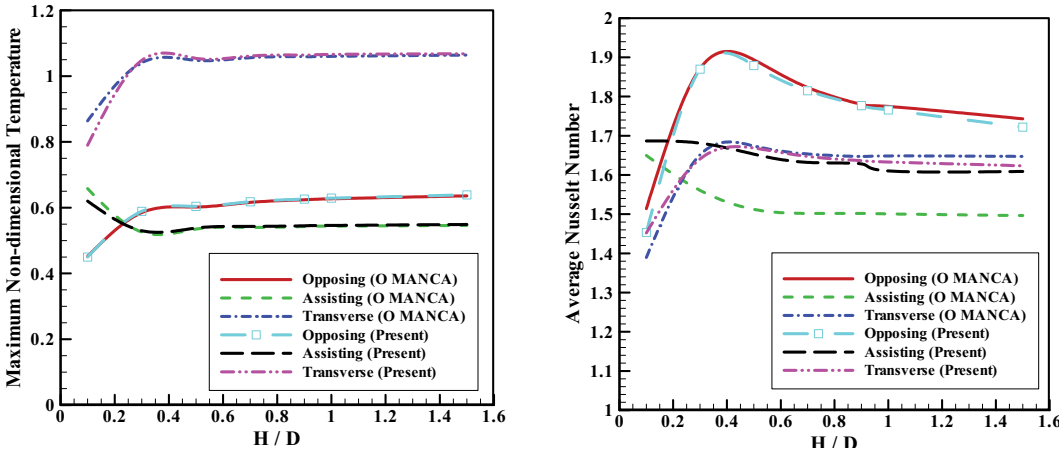

Figure 12: The effect of average Nusselt number on various Ri for different ventilation ratios (a) Assisting forced flow, (b) Opposing forced flow (c) Transverse flow at $Re = 100$.

of their work. In general, the change in maximum dimensionless temperature and average Nusselt number with ventilation ratio is not significant after $H/D \sim 0.4$ at the lower value of Richardson number. Opposing flow case shows the optimum thermal performance while the diffusion effect is dominant.

The Richardson number has significant influence on the average Nusselt number for different ventilation ratios as shown in Fig. 12. In general, the average Nusselt number increases with an increase of Richardson number. Only the opposing forced flow case in Fig. 12(b) shows an idiosyncratic thermal behavior for all values of ventilation ratio except H/D = 0.1. The average Nusselt number is invariant while Richardson number ranges from 0.1 to 0.5 and then decreases slightly up to Ri = 1. Further increase in Richardson number pulls up the average Nusselt number.

5 Heat Transfer Correlations

The average Nusselt numbers can be correlated in terms of Richardson number and the ratio of height of inflow to the length of heat source for Re = 100. These correlations read: Assisting Forced Flow

$$Nu_{av} = 1.990694 Ri^{0.0862651} (H/D)^{0.0439416}$$

for $0.1 \leq Ri \leq 100$ and $0.1 \leq H/D \leq 1.5$; $R^2 =$ 92.46658%

Opposing Forced Flow

$$Nu_{av} = 0.0010344 Ri^{-0.0648389} (H/D)^{6.049938} - .0010344 Ri + 1.56158$$

for $0.1 \leq Ri \leq 100$ and $0.1 \leq H/D \leq 1.5$; $R^2 =$ 85.8857%

Transverse flow

$$Nu_{av} = 2.0577 Ri^{0.1146} (H/D)^{-0.0135}$$

for $0.1 \leq Ri \leq 10$ and $0.3 \leq H/D \leq 1.5$; $R^2 =$ 99.08%

6 Conclusion

Two dimensional numerical investigation of thermal and flow features of mixed convection in a rectangular open cavity has been carried out by using the finite element method. The computational results have been shown for three heating modes. The conclusions of the study can be summarized as follows:

1. At relatively low values of the Richardson number, diffusion is the heat transfer mechanism whereas at higher Richardson numbers, buoyancy driven convection plays an important role. Consequently no significant changes in the average Nusselt number are found for the diffusion dominated case whereas an impetuous increase in average Nusselt number with Richardson number occurs for the convection dominated case. A better heat transfer phenomenon is observed for the transverse flow case at higher values of Richardson number whereas it is obtained for the opposing forced flow case at low Richardson number.

2. A moderate ventilation ratio ($H/D \sim 0.5$) for all cases gives a good thermal performance.

References

Hsu,T. H.; Hsu, Pao-Tung; How, Sey-Ping (1997): Mixed convection in a partially divided rectangular enclosure. *Numerical Heat Transfer*, Part A, vol.31, pp. 655-683.

Hsu, T. H.; Wang, S. G. (2000): Mixed Convection in a Rectangular Enclosure with Discrete Heat Sources. *Numerical Heat Transfer*, Part A, vol. 38, pp. 627-652.

Khanafer, K.; Vafai, K. (2000): Buoyancy-Driven Flow and Heat Transfer in Open-Ended Enclosures: Elimination of the Extended Boundaries. *Int. J. Heat Mass Transfer*, vol. 43, pp. 4087-4100.

Khanafer, K.; Vafai, K.; Lightstone, M. (2002): Mixed convection heat transfer in two dimensional open ended enclosures. *International Journal of Heat and Mass Transfer*, pp. 5171-5190.

Lappa, M. (2005): On the nature and structure of possible three-dimensional steady flows in closed and open parallelepipedic and cubical containers under different heating conditions and driving

forces, *FDMP: Fluid Dynamics & Materials Processing*, Vol. 1, No. 1, pp. 1-19.

Manca, O.; Nardini, S.; Khanafer, K.; Vafai, K. (2003): Effect of heated wall position on mixed convection in a channel with an open cavity. *Numerical Heat Transfer*, Part A, 43(2003), pp. 259-282.

Melnikov, D. E.; Shevtsova, V. M. (2005): Liquid Particles Tracing in Three-dimensional Buoyancy-driven Flows, *FDMP: Fluid Dynamics & Materials Processing*, Vol. 1, No. 2, pp. 189-200.

Omri, A.; Nasrallah, S. B. (1999): Control volume finite element numerical simulation of mixed convection in an air cooled cavity. *Numerical Heat Transfer*, Part A, vol. 36, pp. 615-637.

Oosthuizen, P. H.; Paul, J. T. (1985): Mixed Convective Heat Transfer in a Cavity. *ASME-HTD*, vol. 42, pp. 159-169.

Papanicolaou, E.; Jaluria, Y. (1990): Mixed Convection from an Isolated Heat Source in a Rectangular Enclosure. *Numerical Heat Transfer*, Part A, vol. 18, pp. 427-461.

Papanicolaou, E.; Jaluria, Y. (1993): Mixed Convection from a Localized Heat Source in a Cavity with Conducting Walls: A Numerical Study. *Numerical Heat Transfer*, Part A, vol. 23, pp. 463-484.

Punjabi S.; Muralidhar K.; Panigrahi P.K. (2006): Influence of Layer Height on Thermal Buoyancy Convection in A System with Two Superposed Fluids Confined in A Parallelepipedic Cavity, *FDMP: Fluid Dynamics & Materials Processing*, Vol. 2, No. 2, pp. 95-106.

Sohail, M. and Saghir, M. Z. (2006): Three-Dimensional Modeling of the Effects of Misalignment on the Growth of Ge1-xSix by The Traveling Solvent Method, *FDMP: Fluid Dynamics & Materials Processing*, Vol. 2, No.2, pp.127-140.

Vafai, K.; Ettefagh, J. (1990): Thermal and Fluid Flow Instabilities in Buoyancy-Driven Flows in Open-Ended Cavities. *Int. J. Heat Mass Transfer*, vol. 33, pp. 2329-2344.

Vafai, K.; Desai, C. P.; Iyer, S. V.; Dyko, M. P. (1997): Buoyancy Induced Convection in a Narrow Open-Ended Annulus, *ASME J. Heat Transfer*, vol. 119, pp. 483-494.